The role of aberrations in the relative illumination of a lens system

Dmitry Reshidko* and Jose Sasian
College of Optical Sciences, University of Arizona, Tucson, AZ, 85721, USA

ABSTRACT

Several factors impact the light irradiance and relative illumination produced by a lens system at its image plane. In addition to the cosine-fourth-power radiometric law, image and pupil aberrations, and light vignetting also count. In this paper, we use an irradiance transport equation to derive a closed form solution that provides insight into how individual aberration terms affect the light irradiance and relative illumination. The theoretical results are in agreement with real ray tracing.

Keywords: Relative illumination, irradiance transport, aberration theory, lens design

1. INTRODUCTION

The distribution of light at the focal plane of an optical system is an important aspect of a lens performance. Joseph Petzval was well aware of the image plane illumination and back in 1858 stated, "A third quality of the new combination of lenses is the equal strength of light from the center to the utmost corners of a surface of the image [1]..." The term relative illumination was used as early as the 1900's, when photographers were concerned with the non-uniform illumination in different regions of the negative [2-3]. In the 1950s, the increasing demand for wide-angle lenses used for aerial photography and other purposes renewed interest in the subject. It was found that the decrease in relative illumination of wide-angle lenses limited the angle of view of the early objectives to approximately 95°-105°. The interest in creating accurate topographic maps led to the development of new lens design solutions capable of producing usable imagery over a greater angular field of view [4].

Relative illumination is defined as the ratio of the irradiance in the focal plane at off-axis field positions to the irradiance at the center of the field. The relationship between the illumination and the field angle is derived from basic radiometric principles. For many practical purposes, the $\cos^4$-law has been considered a reasonable approximation to the illumination fall-off produced by a lens at its focal plane; however, assumptions involved in the derivation of the $\cos^4$-law are often found to be incorrectly interpreted in the optical literature [5].

The $\cos^4$-law states that the irradiance of different parts of the image formed by the optical system vary as the fourth power of the cosine of the chief ray angle in object space. As some topographic lenses were found to not follow the $\cos^4$-law the difference was referred to as the 'lens effect' [4]. Reiss showed that the $\cos^4$-law is precisely followed only by an optical system corrected for all image aberrations with an aperture stop that precedes the lens and the object at infinite distance [6]. Other authors emphasize the importance of considering the effect of pupil aberrations and stop position on the illumination. It was found that it is possible to design a lens system in such a way that the decrease in illumination towards the edge of the field occurs more gradually than the $\cos^4$-law [7-9].

In 1946, Roossinov patented a wide-angle lens that instead of the $\cos^4$-law realized a $\cos^3$-law. The area of the entrance aperture of this objective increases towards the edge of the field of view. This phenomenon is achieved by maximum divergence from Abbe's conditions of sines for the front half of the objective, with the object located in the plane of the diaphragm [10].

In 1986, Rimmer outlined a method to accurately calculate relative illumination by real ray tracing. His method is based upon the theory developed by Hopkins and requires determining the size of the exit pupil in the direction cosine space [11, 12]. Similar computation methods of relative illumination are used in modern lens design software [13].

Although it is well known that the relative illumination in an optical system is a function of many variables, there is still confusion regarding the specific role of distortion, pupil aberrations and aperture stop position on the distribution of light at the focal plane. In this paper, we use an irradiance transport equation to derive a closed form solution that approximates to fourth-order the image illumination fall-off and accounts for the illumination effects of aberrations in an

*dmitry@optics.arizona.edu

Novel Optical Systems Design and Optimization XIX, edited by Arthur J. Davis, Cornelius F. Hahlweg, Joseph R. Mulley, Proc. of SPIE Vol. 9948, 994806 · © 2016 SPIE
CCC code: 0277-786X/16/$18 · doi: 10.1117/12.2237204

unvignetted optical system. The role of individual aberration terms on the irradiance distribution at the focal plane is discussed and the results are in agreement with real ray tracing.

2. RADIATIVE TRANSFER IN AN OPTICAL SYSTEM

In this section, we review the radiometry of an optical system. Fig. 1 illustrates the basic elements of an axially symmetric optical system and the geometry defining the transfer of radiant energy. Rays from a differential area dA in object plane pass through the optical system and converge at the conjugate area dA' in the image plane. We define an arbitrary plane S in object space and a plane S' conjugate to S in image space. Differential cross sections of the beam dS in S and dS' in S' are conjugate.

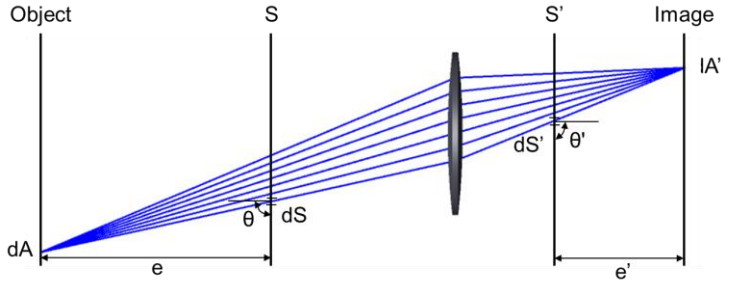

Figure 1. Geometry defining the transfer of radiant energy from differential area dA in object space to the conjugate area dA' in image space. The radiant flux through all cross sections of the beam is the same.

In a lossless and passive optical system, the element of radiant flux $d\Phi$ is conserved through all cross sections of the beam. If we choose planes S and S' at the entrance and exit pupils respectively, the radiative transfer equation becomes

$$d\Phi_{o\to EP} = \frac{L_o}{n_o^{\,2}} \frac{dA\,dS\cos^4(\theta)}{e^2} = \frac{L_o}{n_o^{\,2}} \frac{dA'\,dS'\cos^4(\theta')}{e'^2} = d\Phi_{XP\to i}, \tag{1}$$

where L_o is the source radiance and n_o is the index of refraction in object space. We assume that the source is Lambertian and, consequently, L_o is constant. The object space angle θ is formed between the ray connecting dA and dS, and the optical axis of the lens. Similarly, θ' is the image space angle between the ray connecting dA' and dS', and the optical axis. e' (e) is the axial distance between the object (image) plane and the entrance (exit) pupil plane respectively.

The irradiance is obtained by dividing the radiant flux that is incident on a surface by the unit area. It follows that

$$dE = \frac{d\Phi_{o\to EP}}{dA} = \frac{L_o}{n_o^{\,2}} \frac{dS}{e^2} \cos^4(\theta) \tag{2}$$

and

$$dE' = \frac{d\Phi_{XP\to i}}{dA'} = \frac{L_o}{n_o^{\,2}} \frac{dS'}{e'^2} \cos^4(\theta'), \tag{3}$$

where dE the differential of irradiance in the object plane, dE' is the differential of irradiance at the conjugate point in the image plane. If an optical system is corrected for all image aberrations then the irradiance at the object and image planes are related by the first order transverse magnification m,

$$dE' = \frac{dE}{m^2}. \tag{4}$$

For an optical system with the finite aperture, the irradiance at any point is obtained by integrating Eq. 2 or Eq. 3 over the area of the pupil as

$$E = \int_{EP} \frac{d\Phi_{o\to EP}}{dA} = \frac{L_0}{n_0{}^2 e^2} \int_{EP} dS \cos^4(\theta) \tag{5}$$

and

$$E' = \int_{XP} \frac{d\Phi_{XP\to i}}{dA'} = \frac{L_0}{n_0{}^2 e'^2} \int_{XP} dS' \cos^4(\theta'). \tag{6}$$

If no aberrations are present, the image space irradiance distribution may be evaluated using Eq. 4 as

$$E' = \frac{E}{m^2}. \tag{7}$$

Eq. 5-6 are general and do not involve any approximations. However, care must be used in evaluating these expressions, since the angles θ and θ' are functions of the field and pupil coordinates and may vary due to aberrations. In addition, the boundary of the area over which the integration is extended may also vary for different points in the field of the lens.

3. IRRADIANCE FUNCTION

In this section, we define the irradiance function, $E'(\vec{H},\vec{\rho})$, and show how aberrations are related to the irradiance distribution at the focal plane of an optical system. The irradiance function gives the relative irradiance of the beam at the image plane as a function of the normalized field, $\vec{H}$, and aperture, $\vec{\rho}$, vectors. The field vector lies in the object plane and the aperture vector may be defined in either entrance or exit pupil planes. Two vectors uniquely specify any ray propagating in the lens system. For an axially symmetrical optical system, in analogy with the aberration function, the irradiance function can be expressed as a polynomial. In the limit of small aperture and to the fourth-order of approximation, the irradiance function is [14]

$$E'(\vec{H},\vec{\rho}) = \mathrm{E'}_{000} + \mathrm{E'}_{200}(\vec{H}\cdot\vec{H}) + \mathrm{E'}_{400}(\vec{H}\cdot\vec{H})^2. \tag{8}$$

This derivation implies that the irradiance is greater than zero for any point defined by the normalized field $\vec{H}$ and aperture $\vec{\rho}$ vectors.

3.1 Thin Ideal Lens with the Stop Aperture at the Lens.

If the aperture stop is located at a thin ideal (no aberrations) lens, then both entrance (EP) and exit (XP) pupils coincide at the lens. The differential areas dS and dS' are equal and constant by construction. A point in the object plane defined by the field vector, $\overrightarrow{H}$, is imaged ideally into a point in the image plane also defined by $\overrightarrow{H}$.

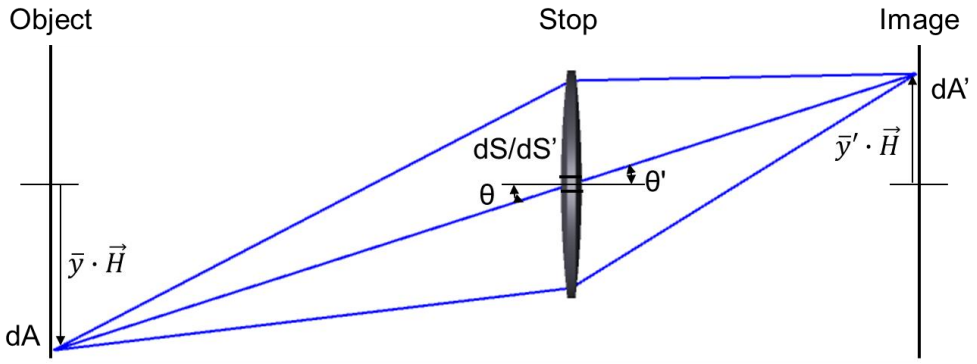

Figure 2. Geometrical variables involved in computing irradiance at the focal plane of a thin ideal, aberration free lens with the stop at the lens.

In the limit of a small aperture, the variation of irradiance across the image plane is given by Eq. 3. We consider the irradiance contribution of the on-axis differential area at the stop to the image point defined by the field vector $\vec{H}$ and express the cosine as a function of the field vector. We use a Taylor series expansion to show that to the fourth-order of approximation the cosine-to-the-fourth-power of the angle between the ray connecting these two points and the optical axis is given by

$$\cos^4(\theta') = [1 - 2 \cdot \bar{u}'^2 (\vec{H} \cdot \vec{H}) + 3 \cdot \bar{u}'^4 (\vec{H} \cdot \vec{H})^2], \tag{9}$$

where $\bar{u}'$ is the chief ray slope in image space. We substitute Eq. 9 into Eq. 3 and write the irradiance at the image plane of the ideal lens with the stop at the lens as

$$I'_{0/ideal} \equiv \frac{L_o}{n_o^2} \frac{dS'}{e'^2} \tag{10}$$

and

$$E'_{ideal}(\vec{H}) = I'_0 \cdot [1 - 2 \cdot \bar{u}'^2 (\vec{H} \cdot \vec{H}) + 3 \cdot \bar{u}'^4 (\vec{H} \cdot \vec{H})^2], \tag{11}$$

where $I'_{0/ideal}$ is the irradiance value for the on-axis field point. We divide Eq. 11 by Eq. 10 to obtain the relative illumination

$$Ri_{ideal}(\vec{H}) = 1 - 2 \cdot \bar{u}'^2 (\vec{H} \cdot \vec{H}) + 3 \cdot \bar{u}'^4 (\vec{H} \cdot \vec{H})^2 . \tag{12}$$

Eq. 12 is equivalent to the fourth-order expansion of the cos^4-law in terms of first-order quantities. The irradiance at the image plane can also be computed by substituting Eq. 2 into Eq. 4 and evaluating the cosine function in object space. In the simple case of an ideal lens with the stop at the lens, the chief rays slopes in image and object spaces are equal: $\bar{u} = \bar{u}'$. Then we can recover Eq. 12 by starting the calculation in either object or image space.

3.2 Stop Aperture Follows the Lens

If the aperture stop of the system follows the lens, then the XP is the actual physical diaphragm. By construction, beams at the XP are uniform given that we choose to define rays at the exit pupil. For this example, it is easier to integrate Eq. 6 because of the simple limits of integration or use Eq. 3 in the limit of a small aperture. By contrast to the previous case, in an actual system rays may not pass through the ideal image point due to aberrations as shown in Fig. 3. The ray intersection with the image plane is determined by considering the transverse ray errors $\Delta\vec{H}$ and it is defined by the vector $\vec{H} + \Delta\vec{H}$.

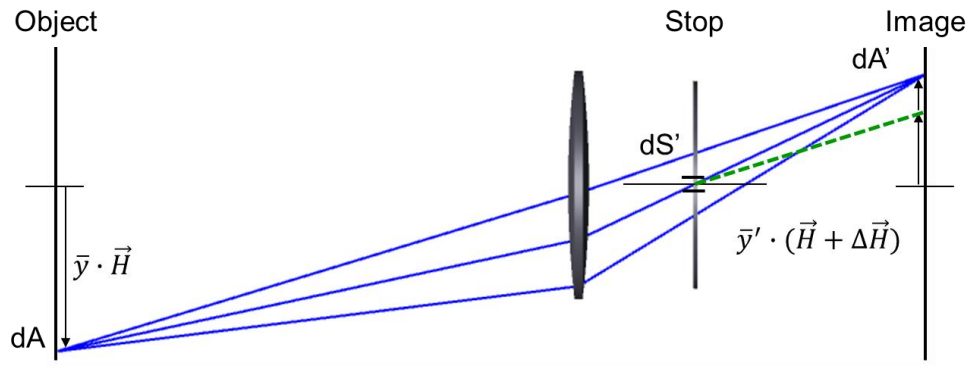

Figure 3. Geometrical variables involved in computing irradiance at the focal plane of the optical system with the aperture stop that follows the lens. Real rays (solid lines) and first-order rays (dashed lines) coincide at the exit pupil. Real rays may not pass through the ideal image point due to aberrations.

In the presence of image aberrations, Eq. 6 determines the irradiance function $E'(\vec{H}+\Delta\vec{H},\vec{\rho})$ at point $\vec{H}+\Delta\vec{H}$ of the image and coordinate $\vec{\rho}$ at the exit pupil. We write the differential of irradiance at the image as

$$E'(\vec{H}+\Delta\vec{H},\vec{\rho}) \simeq E'(\vec{H},\vec{\rho}) + \nabla_H E'(\vec{H},\vec{\rho})\cdot\Delta\vec{H}\,, \tag{13}$$

where $\nabla_H E'(\vec{H},\vec{\rho})$ is the gradient of the irradiance function with the respect to the field vector $\vec{H}$. With no second-order terms in the aberrations function, the terms $\nabla_H E'(\vec{H},\vec{\rho})\cdot\Delta\vec{H}$ result in irradiance terms that are at least of fourth-order. In the limit of a small aperture for a system with distortion the transverse ray errors to the third-order become

$$\Delta\vec{H} = -\frac{1}{\mathcal{K}} W_{311}(\vec{\mathrm{H}}\cdot\vec{\mathrm{H}})\,\vec{\mathrm{H}}\,. \tag{14}$$

By combining Eq. 11, Eq. 13 and Eq. 14, and evaluating at the limit of small aperture, the relative illumination of the lens system with the stop that follows the lens is

$$Ri_{XP}(\vec{H}) = 1 - 2\cdot\bar{u}'^2(\vec{\mathrm{H}}\cdot\vec{\mathrm{H}}) + [3\cdot\bar{u}'^4 + \frac{4}{\mathcal{K}} W_{311}\cdot\bar{u}'^2](\vec{\mathrm{H}}\cdot\vec{\mathrm{H}})^2 = Ri_{ideal} + \frac{4}{\mathcal{K}} W_{311}\cdot\bar{u}'^2(\vec{\mathrm{H}}\cdot\vec{\mathrm{H}})^2\,. \tag{15}$$

Thus, we conclude that the second-order relative illumination term is not affected by image distortion aberration W_{311}. The third-order distortion contributes to the fourth-order relative illumination coefficient. When negative "barrel" distortion is present, the irradiance over the field is more uniform than when the distortion is absent.

3.3 Stop Aperture Precedes the Lens

For this case, the EP is the actual physical diaphragm in the optical system. In the limit of small aperture, with the aperture vector $\vec{\rho}$ set at the EP and no image aberrations, Eq. 2 and Eq. 4 determine the irradiance distribution at the focal plane. The expression for the relative illumination will be similar to Eq. 8, except the object space ray slopes are substituted with image space ray slopes

$$Ri_{EP}(\vec{H}) = 1 - 2\cdot\bar{u}^2(\vec{\mathrm{H}}\cdot\vec{\mathrm{H}}) + 3\cdot\bar{u}^4(\vec{\mathrm{H}}\cdot\vec{\mathrm{H}})^2\,. \tag{16}$$

For the system with aberrations, on the other hand, we must use Eq. 3. The exit pupil now is a distorted image of the entrance pupil and the ray angle in Eq. 3 is determined by considering the transverse ray errors at both the image and exit pupil planes as shown in Fig. 4.

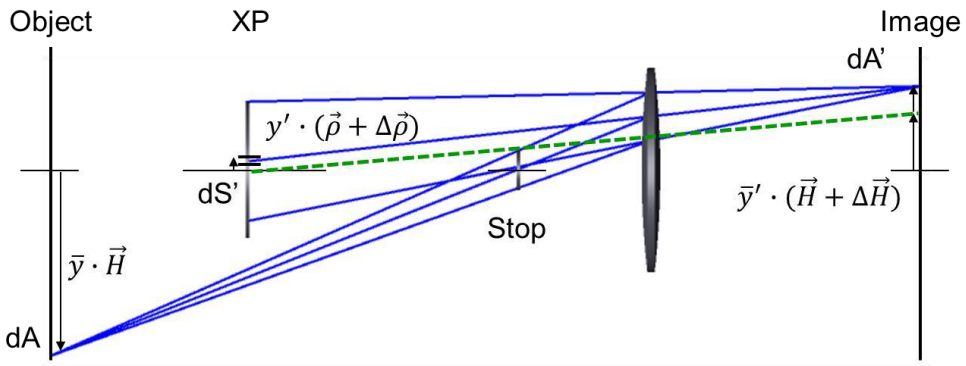

Figure 4. Geometrical variables involved in computing irradiance at the focal plane of the optical system with the aperture stop that precedes the lens. Real rays (solid lines) and first-order rays (dash lines) coincide at the entrance pupil. Real rays may not pass through the ideal point at both exit pupil and image planes due to aberrations.

The irradiance function $E'(\vec{H}+\Delta\vec{H}, \vec{\rho}+\Delta\vec{\rho})$ is evaluated at the image point defined by the vector $\vec{H}+\Delta\vec{H}$ and the coordinate at the exit pupil defined by the vector $\vec{\rho}+\Delta\vec{\rho}$. We can write for the differential of irradiance at the image plane as

$$E'(\vec{H}+\Delta\vec{H}, \vec{\rho}+\Delta\vec{\rho}) \simeq E'(\vec{H}, \vec{\rho}) + \nabla_H E'(\vec{H}, \vec{\rho}) \cdot \Delta\vec{H} + \nabla_\rho E'(\vec{H}, \vec{\rho}) \cdot \Delta\vec{\rho}\,, \tag{17}$$

where $\nabla_H E'(\vec{H}, \vec{\rho})$ and $\nabla_\rho E'(\vec{H}, \vec{\rho})$ are the gradients of the irradiance function with respect to the field $\vec{H}$ and aperture $\vec{\rho}$ vectors respectively.

Moreover, if the differential area dS' in Eq. 3 is an image of the differential area dS, then the size of dS' may also vary over the exit pupil and over the field due to pupil aberrations. Two differential areas are related by the determinant of the Jacobian of the transformation

$$dS' = J(\vec{H}, \vec{\rho})dS\,. \tag{18}$$

We substitute Eq. 18 into Eq. 3 to find

$$dE'(\vec{H}, \vec{\rho}) = \frac{L_0}{n_0^{\,2} e'^2} dS' \cos^4(\theta') = \frac{L_0 dS}{n_0^{\,2} e'^2} \cdot \mathrm{J}(\vec{H}, \vec{\rho}) \cdot \cos^4(\theta') = I'_{0/XP} \cdot \mathrm{J}(\vec{H}, \vec{\rho}) \cdot \cos^4(\theta')\,, \tag{19}$$

where $I'_{0/XP}$ is the irradiance value for the on axis field point. To obtain the Jacobian determinant we express the transverse pupil ray aberration vector $\Delta\vec{\rho}$ in orthogonal components along unit vectors $\vec{h}$ and $\vec{k}$ as

$$\Delta\vec{\rho} = \Delta\rho_k \vec{k} + \Delta\rho_h \vec{h}\,, \tag{20}$$

where $\vec{h}$ is a unit vector along the field vector $\vec{H}$ and $\vec{k}$ is a unit vector perpendicular to the field vector $\vec{H}$. Then, we consider the transformations $\rho'_h = \rho_h + \Delta\rho_h$ and $\rho'_k = \rho_k + \Delta\rho_k$, which gives the position of the given ray at the exit pupil, and so we find the Jacobian determinant

$$J(\vec{H}, \vec{\rho}) = \frac{y'^2_{XP}}{y^2_{EP}} \left(1 + \nabla_\rho \Delta\vec{\rho} + \frac{\partial\Delta\vec{\rho}_h}{\partial\vec{\rho}_h}\frac{\partial\Delta\vec{\rho}_k}{\partial\vec{\rho}_k} - \frac{\partial\Delta\vec{\rho}_h}{\partial\vec{\rho}_k}\frac{\partial\Delta\vec{\rho}_k}{\partial\vec{\rho}_h}\right), \tag{21}$$

where $\nabla_\rho \Delta\vec{\rho}$ is the divergence of the transverse pupil ray error [14, 15]. We substitute Eq. 19 and Eq. 21 into Eq. 17, and neglecting six-order terms the expression for the distribution of the irradiance at the focal plane becomes

$$E'(\vec{H}+\Delta\vec{H},\vec{\rho}+\Delta\vec{\rho}) \simeq E'(\vec{H},\vec{\rho}) + \nabla_H E'(\vec{H},\vec{\rho})\cdot\Delta\vec{H} + \nabla_\rho E'(\vec{H},\vec{\rho})\cdot\Delta\vec{\rho}$$
$$+E'(\vec{H},\vec{\rho})[\nabla_\rho\Delta\vec{\rho} + \frac{\partial\Delta\vec{\rho}_h}{\partial\vec{\rho}_h}\frac{\partial\Delta\vec{\rho}_k}{\partial\vec{\rho}_k} - \frac{\partial\Delta\vec{\rho}_h}{\partial\vec{\rho}_k}\frac{\partial\Delta\vec{\rho}_k}{\partial\vec{\rho}_h}]. \tag{22}$$

With no second order terms in the aberration function, the terms $\nabla_H E'(\vec{H},\vec{\rho})\cdot\Delta\vec{H}$ and $\nabla_\rho E'(\vec{H},\vec{\rho})\cdot\Delta\vec{\rho}$ result in irradiance terms that are at least of fourth-order. The terms $[\nabla_\rho\Delta\vec{\rho} + \frac{\partial\Delta\vec{\rho}_h}{\partial\vec{\rho}_h}\frac{\partial\Delta\vec{\rho}_k}{\partial\vec{\rho}_k} - \frac{\partial\Delta\vec{\rho}_h}{\partial\vec{\rho}_k}\frac{\partial\Delta\vec{\rho}_k}{\partial\vec{\rho}_h}]$ are at least of second-order and once multiplied by $E'(\vec{H},\vec{\rho})$ reveal second- and fourth-order terms. In the limit of small aperture, only pupil spherical aberration and pupil coma contribute irradiance terms. The relationships between pupil wavefront deformations and transverse pupil aberrations to fifth-order are given by Sasian [16]:

$$\Delta\vec{\rho} = \frac{4}{\mathcal{H}}\overline{W}_{040}(\vec{H}\cdot\vec{H})\vec{H} + \frac{1}{\mathcal{H}}\overline{W}_{131}[(\vec{H}\cdot\vec{H})\vec{\rho} + 2(\vec{H}\cdot\vec{\rho})\vec{H}]$$
$$+\frac{1}{\mathcal{H}}\overline{W}_{151}[(\vec{H}\cdot\vec{H})^2\vec{\rho} + 4(\vec{H}\cdot\vec{H})(\vec{H}\cdot\vec{\rho})\vec{H}]$$
$$+\frac{1}{\mathcal{H}}[5\cdot\overline{W}_{131}\cdot\overline{u}'^2 + 4\cdot\overline{W}_{040}\cdot\overline{u}'u'](\vec{H}\cdot\vec{H})^2\vec{\rho}$$
$$-\frac{1}{\mathcal{H}}[4\cdot\overline{W}_{131}\cdot\overline{u}'^2 + 8\cdot\overline{W}_{040}\cdot\overline{u}'u'](\vec{H}\cdot\vec{H})(\vec{H}\cdot\vec{\rho})\vec{H}$$
$$-\frac{1}{\mathcal{H}^2}\left[8\overline{W}_{040}W_{220} + 2\overline{W}_{131}W_{311}\right](\vec{H}\cdot\vec{H})^2\vec{\rho}$$
$$-\frac{1}{\mathcal{H}^2}\left[24\overline{W}_{040}W_{220} + 16\overline{W}_{040}W_{222} + 4\overline{W}_{131}W_{311}\right](\vec{H}\cdot\vec{H})(\vec{H}\cdot\vec{\rho})\vec{H}. \tag{23}$$

The fifth-order transverse pupil ray errors in Eq. 23 include extra terms that are products of fourth-order pupil aberration coefficients and the paraxial ray slopes $\overline{u}'$ and u' in the image space as well as terms that are products of the fourth-order image and pupil aberrations. By substituting Eq. 14 and Eq. 23 into Eq. 22 and taking the required derivatives, we find that in the limit of small aperture the relative illumination of the lens system with the stop that precedes the lens is

$$Ri_{EP}(\vec{H}) \simeq 1 + [-2\overline{u}'^2 + \frac{4}{\mathcal{H}}\overline{W}_{131}](\vec{H}\cdot\vec{H})$$
$$+[3\overline{u}'^4 + \frac{4}{\mathcal{H}}W_{311}\overline{u}'^2 + \frac{6}{\mathcal{H}}\overline{W}_{151} - \frac{3}{\mathcal{H}}\overline{W}_{131}\overline{u}'^2](\vec{H}\cdot\vec{H})^2$$
$$-\frac{1}{\mathcal{H}^2}\left[32\overline{W}_{040}W_{220} + 24\overline{W}_{040}W_{222} + 8\overline{W}_{131}W_{311}\right](\vec{H}\cdot\vec{H})^2$$
$$+\frac{3}{\mathcal{H}^2}\overline{W}_{131}\overline{W}_{131}(\vec{H}\cdot\vec{H})^2. \tag{24}$$

The residual field curvature and astigmatism of an objective lens that produces sharp imaging on a flat surface are small and additional terms that are products of these aberrations and pupil aberrations may be neglected. The fourth- and sixth-order pupil comas, $\overline{W}_{131}$ and $\overline{W}_{151}$ respectively, produce the aspect ratio change in the cross-section of the beam at the

exit pupil as shown in Fig. 5. By controlling pupil coma during the lens design process it is possible to change the effective exit pupil area for off-axis field points and increase the amount of light accepted by the objective. This is known as Slyusarev effect. In the presence of pupil spherical aberration $\bar{W}_{040}$, the beam at the exit pupil changes position laterally along different points in the field-of-view. However, it should be noted that when the stop precedes a lens and $W_{220} = W_{222} = 0$, spherical aberration of the pupil does not affect the relative illumination to fourth-order, though it may change the chief ray angle of incidence at the image plane.

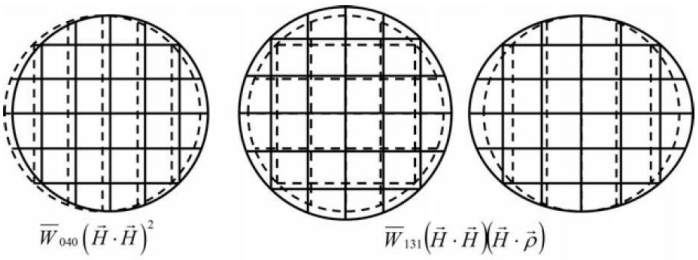

Figure 5. Pupil grid mapping effects due to pupil aberrations in relation to ideal pupil (broken line). Pupil coma may change the area of the pupil, whereas pupil spherical aberration may shift transversely the pupil [16].

The fourth-order pupil coma and image distortion are directly related:

$$\bar{W}_{131} = W_{311} - \frac{\mathcal{K}}{2}\Delta\{\bar{u}^2\}, \tag{25}$$

and to the second-order, the relative illumination in terms of object space slopes is

$$Ri_{EP}(\vec{H}) \simeq 1 + [-2\bar{u}^2 + \frac{4}{\mathcal{K}}W_{311}](\vec{H}\cdot\vec{H}). \tag{26}$$

The fourth order expression for the relative illumination in terms of object space quantities is more complicated and does not provide additional insight. Finally, we compare Eq. 24 to Eq. 15 to show extra relative illumination terms that emerge from switching the aperture stop from the exit pupil to the entrance pupil. In the limit of small aperture and $W_{220} = W_{222} = 0$, the relative illumination becomes

$$\begin{aligned} Ri_{EP}(\vec{H}) &\simeq Ri_{XP}(\vec{H}) + \frac{4}{\mathcal{K}}\bar{W}_{131}(\vec{H}\cdot\vec{H}) \\ &+[\frac{6}{\mathcal{K}}\bar{W}_{151} - \frac{3}{\mathcal{K}}\bar{W}_{131}\bar{u}'^2 - \frac{8}{\mathcal{K}^2}\bar{W}_{131}W_{311} + \frac{3}{\mathcal{K}^2}\bar{W}_{131}\bar{W}_{131}](\vec{H}\cdot\vec{H})^2. \end{aligned} \tag{27}$$

If the aperture stop precedes the lens, it is possible to have sufficient pupil aberrations such that the illumination will be more uniform or even constant over the entire field.

3.4 Stop Aperture between Components of the Lens

In order to derive an expression for the image plane illumination of a lens system with an internal diaphragm, we divide the lens into two parts and evaluate the contribution of each part. Part A consists of all optical elements between the object plane and the diaphragm and thus has the aperture stop at the exit pupil. Part B includes all elements between the diaphragm and the image plane and has the aperture stop at the entrance pupil. By construction, the exit pupil of part A is the entrance pupil of part B. Furthermore, the image formed by A is the object of B.

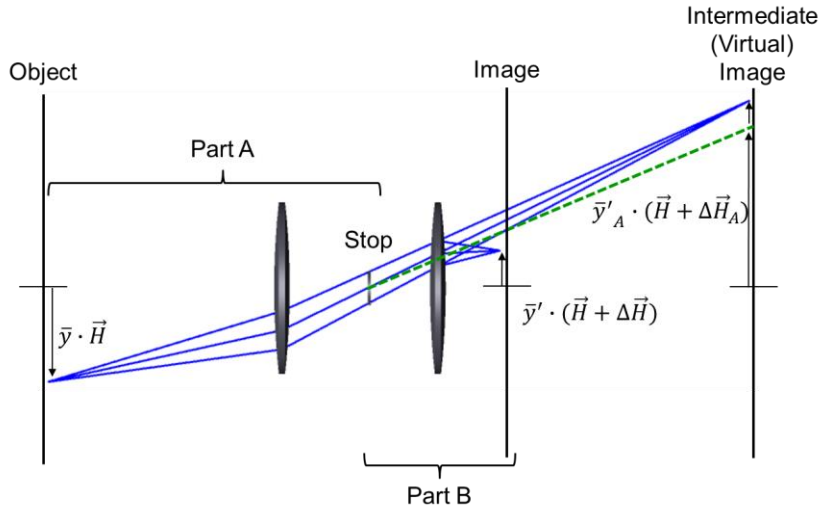

Figure 6. Geometrical variables involved in computing irradiance at the focal plane of the optical system with the aperture stop between components the lens. The lens is divided into two parts A and B and contributions of each part are evaluated individually.

If part A is corrected for all image aberrations, the beams after A converge to the image points defined by the field vector $\vec{H}$. The incoming beams incident on part B have no aberrations and in the limit of small aperture relative illumination of the system is given by the expression similar to Eq. 24

$$\begin{aligned} Ri_{EP}(\vec{H}) \simeq 1 + [-2\bar{u}'^2 + \frac{4}{\mathcal{H}}\bar{W}_{131B}](\vec{H}\cdot\vec{H}) \\ [3\bar{u}'^4 + \frac{4}{\mathcal{H}}W_{311B}\bar{u}'^2 + \frac{6}{\mathcal{H}}\bar{W}_{151B} - \frac{3}{\mathcal{H}}\bar{W}_{131B}\bar{u}'^2](\vec{H}\cdot\vec{H})^2 \\ -\frac{1}{\mathcal{H}^2}\left[32\bar{W}_{040B}W_{220B} + 24\bar{W}_{040B}W_{222B} + 8\bar{W}_{131B}W_{311B}\right](\vec{H}\cdot\vec{H})^2 \\ +\frac{3}{\mathcal{H}^2}\bar{W}_{131B}\bar{W}_{131B}(\vec{H}\cdot\vec{H})^2, \end{aligned} \tag{28}$$

where the subscript B refers to aberration coefficients of part B alone. Most objectives with the internal diaphragm are designed to provide the best image quality only at the system focal plane. Parts A and B of the objective are not corrected individually. Part A forms a highly aberrated image, which is reimaged and compensated by the rest of the system. In the limit of small aperture, the distortion of A contributes transverse ray errors $\Delta\vec{H}_A$ to the third-order given by

$$\Delta\vec{H}_A = -\frac{1}{\mathcal{H}}W_{311A}(\vec{\mathrm{H}}\cdot\vec{\mathrm{H}})\,\vec{\mathrm{H}}\,. \tag{29}$$

The image points of A are now defined by the vector $\vec{H} + \Delta\vec{H}_A$ and the relative illumination of the system is calculated by evaluating Eq. 28 at $Ri_{EP}(\vec{H} + \Delta\vec{H}_A)$. The second-order terms contribute extra fourth-order terms and the expression for the relative illumination of an optical system with internal diaphragm to fourth-order is

$$
\begin{aligned}
Ri_{EP}(\vec{H}) \simeq & 1+[-2\bar{u}'^2+\frac{4}{\mathcal{H}}\bar{W}_{131B}](\vec{H}\cdot\vec{H}) \\
& +[3\bar{u}'^4+\frac{4}{\mathcal{H}}W_{311A}\bar{u}'^2+\frac{4}{\mathcal{H}}W_{311B}\bar{u}'^2+\frac{6}{\mathcal{H}}\bar{W}_{151B}-\frac{3}{\mathcal{H}}\bar{W}_{131B}\bar{u}'^2](\vec{H}\cdot\vec{H})^2 \\
& -\frac{1}{\mathcal{H}^2}\left[32\bar{W}_{040B}W_{220B}+24\bar{W}_{040B}W_{222B}+8\bar{W}_{131B}W_{311B}\right](\vec{H}\cdot\vec{H})^2 \\
& +[\frac{3}{\mathcal{H}^2}\bar{W}_{131B}\bar{W}_{131B}-\frac{8}{\mathcal{H}^2}\bar{W}_{131B}W_{311A}](\vec{H}\cdot\vec{H})^2
\end{aligned}
\tag{30}
$$

A comparision of Eq. 28 and Eq. 30 reveals two additional terms that are casued by the aberrations of part A. The term $\frac{4}{\mathcal{H}}W_{311A}\bar{u}'^2$, combined with the term $\frac{4}{\mathcal{H}}W_{311B}\bar{u}'^2$, results in the total distortion of the system: $\frac{4}{\mathcal{H}}W_{311}\bar{u}'^2$. The term $-\frac{8}{\mathcal{H}^2}\bar{W}_{131B}W_{311A}$ is a product of the pupil aberration of part B and the image aberration of part A. In the special case of an optical system with symmetry around the stop, the distortion of parts A and B has the same magnitude but opposite sign. Moreover, each part of the symmetrical optical system is separetly corrected for field curvature and astigmatism. We substitute $W_{311A}=-W_{311B}$ into Eq. 30 and write a simplified expression for the relative illumination of a symetrical optical system

$$
\begin{aligned}
Ri_{EP}(\vec{H}) \simeq & 1+[-2\bar{u}'^2+\frac{4}{\mathcal{H}}\bar{W}_{131B}](\vec{H}\cdot\vec{H}) \\
& [3\bar{u}'^4+\frac{6}{\mathcal{H}}\bar{W}_{151B}-\frac{3}{\mathcal{H}}\bar{W}_{131B}\bar{u}'^2+\frac{3}{\mathcal{H}^2}\bar{W}_{131B}\bar{W}_{131B}](\vec{H}\cdot\vec{H})^2.
\end{aligned}
\tag{31}
$$

We conclude that the relative illumination of a symetrical optical system does not depend on the aberration contributions of elements that preceed the diaphragm. More uniform illumination at the focal plane can be achieved by controling the pupil coma of the rear part of the system.

3.5 Summary of Relative Illumination Coefficients

Second- and fourth-order relative illumination coefficients for different cases considered in Sections 3.1-3.4 are summarized in Table 1.

Table 1. Summary of second- and fourth-order relative illumination coefficients for different cases. Relative illumination is expressed as a polynomial $Ri(\vec{H}) = 1 + Ri_{200}(\vec{H}\cdot\vec{H}) + Ri_{400}(\vec{H}\cdot\vec{H})^2$.

Case	**2nd order coefficient (Ri_{200})**	**4th order coefficient (Ri_{400})**
Thin Ideal Lens. Stop Aperture at the Lens.	$-2\cdot\bar{u}'^2$	$3\cdot\bar{u}'^4$
Stop Aperture follows the Lens.	$-2\cdot\bar{u}'^2$	$3\cdot\bar{u}'^4 + \frac{4}{\mathcal{J}}W_{311}\cdot\bar{u}'^2$
Stop Aperture precedes the Lens.	$-2\bar{u}'^2 + \frac{4}{\mathcal{J}}\bar{W}_{131}$	$3\bar{u}'^4 + \frac{4}{\mathcal{J}}W_{311}\bar{u}'^2 + \frac{6}{\mathcal{J}}\bar{W}_{151} - \frac{3}{\mathcal{J}}\bar{W}_{131}\bar{u}'^2 + \frac{3}{\mathcal{J}^2}\bar{W}_{131}\bar{W}_{131} - \frac{1}{\mathcal{J}^2}\left[32\bar{W}_{040}W_{220} + 24\bar{W}_{040}W_{222} + 8\bar{W}_{131}W_{311}\right]$
Stop Aperture precedes the Lens. $W_{220} = W_{222} = 0$	$-2\bar{u}'^2 + \frac{4}{\mathcal{J}}\bar{W}_{131}$	$3\bar{u}'^4 + \frac{4}{\mathcal{J}}W_{311}\bar{u}'^2 + \frac{6}{\mathcal{J}}\bar{W}_{151} - \frac{3}{\mathcal{J}}\bar{W}_{131}\bar{u}'^2 - \frac{8}{\mathcal{J}^2}\bar{W}_{131}W_{311} + \frac{3}{\mathcal{J}^2}\bar{W}_{131}\bar{W}_{131}$
Stop Aperture precedes the Lens. No Image Aberrations.	$-2\cdot\bar{u}^2$	$3\cdot\bar{u}^4$
Stop Aperture between Components of the Lens.	$-2\bar{u}'^2 + \frac{4}{\mathcal{J}}\bar{W}_{131B}$	$3\bar{u}'^4 + \frac{4}{\mathcal{J}}W_{311A}\bar{u}'^2 + \frac{4}{\mathcal{J}}W_{311B}\bar{u}'^2 + \frac{6}{\mathcal{J}}\bar{W}_{151B} - \frac{3}{\mathcal{J}}\bar{W}_{131B}\bar{u}'^2 - \frac{1}{\mathcal{J}^2}\left[32\bar{W}_{040B}W_{220B} + 24\bar{W}_{040B}W_{222B} + 8\bar{W}_{131B}W_{311B}\right] + \frac{3}{\mathcal{J}^2}\bar{W}_{131B}\bar{W}_{131B} - \frac{8}{\mathcal{J}^2}\bar{W}_{131B}W_{311A}$
Symmetrical Optical System	$-2\bar{u}'^2 + \frac{4}{\mathcal{J}}\bar{W}_{131B}$	$3\bar{u}'^4 + \frac{6}{\mathcal{J}}\bar{W}_{151B} - \frac{3}{\mathcal{J}}\bar{W}_{131B}\bar{u}'^2 + \frac{3}{\mathcal{J}^2}\bar{W}_{131B}\bar{W}_{131B}$

3.6 Relative Illumination Coefficient Verification

In order to verify the algebraic form of the relative illumination coeffitients, it is desirable to determine their magnitude. A macro program was written to numerically calculate the coefficients by making an iterative fit to a selected set of relative illumination values across the field of view of an optical system. The iterative algorithm is similar to one used by Sasian to fit aberration coefficients [14]. The loop in Table 2 is executed.

Table 2. Iterative algorithm that was used to fit relative illumination coefficients.

FOR $i = 1$ to 100

$H = 0.2$

$Ri = RELI(H)$

$E_{200} = (Ri - 1 - E_{400}H^4 - E_{600}H^6 - E_{800}H^8 - E_{1000}H^{10}) \cdot H^{-2}$

$H = 0.4$

$Ri = RELI(H)$

$E_{400} = (Ri - 1 - E_{200}H^2 - E_{600}H^6 - E_{800}H^8 - E_{1000}H^{10}) \cdot H^{-4}$

$H = 0.6$

$Ri = RELI(H)$

$E_{600} = (Ri - 1 - E_{200}H^2 - E_{400}H^4 - E_{800}H^8 - E_{1000}H^{10}) \cdot H^{-6}$

$H = 0.8$

$Ri = \mathrm{RELI}(H)$

$E_{800} = (Ri - 1 - E_{200}H^2 - E_{400}H^4 - E_{600}H^6 - E_{1000}H^{10}) \cdot H^{-8}$

$H = 1$

$Ri = RELI(H)$

$E_{1000} = (Ri - 1 - E_{200}H^2 - E_{400}H^4 - E_{600}H^6 - E_{800}H^8) \cdot H^{-10}$

NEXT

The quantity $RELI(H)$ is the relative illumination at the specified field computed by real ray tracing in a lens design program. After a few iterations of this loop, the coefficients E_{200} and E_{400} converge to the theoretical values with insignificant error. This iterative fit methodology was used to test the coefficients values at several conjugate distances and aperture stop positions for both single surface and a system of several surfaces. The obvious agreement of the formulas with the coefficients found with the above iterative loop supports the validity of the theory. For example, the relative illumination coefficients for a Landscape lens [18] shown in Fig.7 were calculated both ways. We limit the field of view (FOV) to 30° and close the diaphragm to meet a small aperture approximation. Table 3 presents a comparison of coefficients where the differences in the eighth decimal place are likely due to the computational approach used.

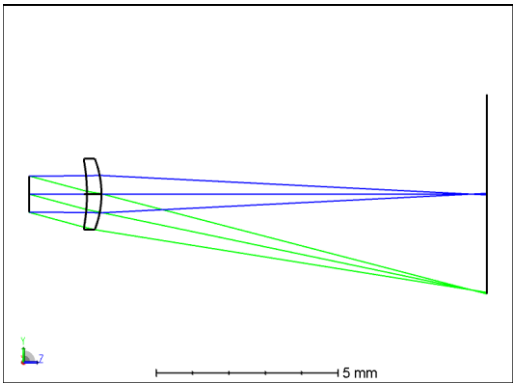

Figure 7. Landscape lens used to compare relative illumination coefficients computed analytically and numerically. In order to minimize fitting errors, the FOV of the lens is limited to 30°.

Table 3. Comparison of relative illumination coefficients computed analytically and numerically. The agreement to eighth digits supports the correctness of the formulas.

Coefficient	Analytical formula	Numerical calculation
E_{200}	-0.1014613*598*	-0.1014613*677*
E_{400}	0.0091763*329*	0.0091763*317*

4. EXAMPLES

In this section, we provide several examples of lenses that, rather than following the standard $\cos^4$-law, showed an improved illumination at the focal plane. Aberration theory is used to provide insight into the role of the individual aberration terms in the relative illumination of these lenses.

4.1 Mobile Phone Camera Lens

Miniature cameras for consumer electronics and mobile phones are a rapidly growing technology. The system level requirements such as manufacturing cost, packaging, and sensor characteristics impose unique challenges for optical designers. Relative illumination is one of the most interesting characteristics of miniature camera lens designs.

The typical distortion requirement in mobile camera lenses is <2% and the FOV is large (common FOV values are 65 - 75°). On the other hand, the chief ray incidence angle (CRA) on the sensor is usually limited to no more than 30°. The CRA impacts the relative illumination, which often is set to 50% at the sensor corners. For better CRA control, the aperture stop in a conventional mobile lens is placed close to the front, away from the image plane. The aperture stop position and the strong aspheric next to the image plane generate exit pupil spherical aberration, which reduces the CRA.

Mobile lenses are well known for the extensive use of aspheric surfaces. The interaction of multiple aspherics within the design enables a high level of control over aberrations. Particularly, sharp imaging on a flat surface can be achieved without satisfying the classical requirement of having a Petzval sum nearly zero. The aspheric optical elements located close to the image plane contribute higher-order field curvature and astigmatism. Different orders of the field curvature and astigmatism are balanced to compensate for any residual Petzval curvature [19].

To illustrate how aberrations affect the relative illumination of a mobile camera lens we evaluate different terms in Eq. 24 for one of the early miniature digital camera patents [20]. The three-element design shown in Fig. 8a covers a FOV of 64° at f/2.8. Field curvature and distortion plots are shown in Fig. 8b. A small positive fourth-order distortion is compensated with a higher-order negative distortion resulting in <0.5% of total distortion. The Petzval radius is about two times the focal length; this clearly indicates that the residual field curvature is compensated by balancing higher orders of the field curvature and astigmatism. Aberration contributions to the relative illumination, sorted in descending order, are summarized in Table 4.

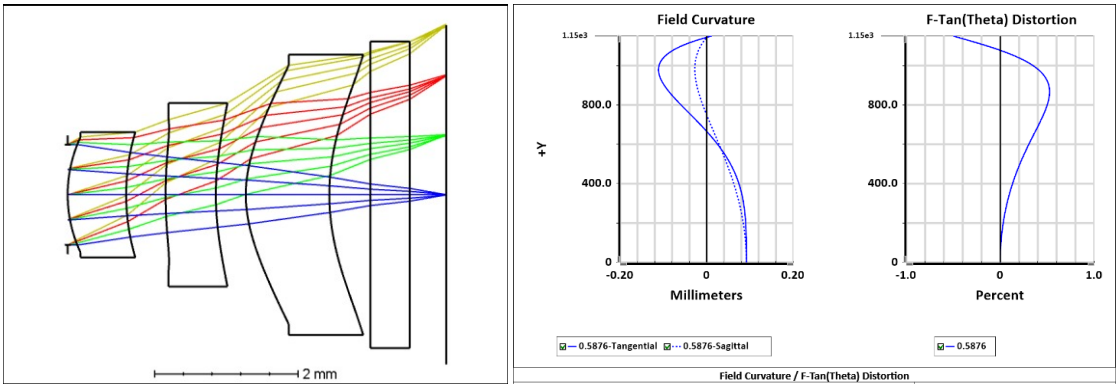

(a) (b)

Figure 8. U.S. Patent 6441971: (a) Layout, (b) field curvature and distortion plot. Distortion correction requirements do not allow one to significantly reduce the chief ray incidence angle on the sensor (CRA). Exit pupil spherical aberration shifts the pupil radially and reduces the CRA. Higher order field curvature and astigmatism are balanced to compensate for the residual Petzval field curvature.

Table 4. Contributions to the relative illumination according to Eq. 24 for US. 6441971.

2nd order coefficient (Ri_{200})	**Numerical value**	**4th order coefficient (Ri_{400})**	**Numerical value**
$-2\bar{u}'^2$	-0.745977	$3\bar{u}'^4$	0.417361
$\frac{4}{Ж}\bar{W}_{131}$	0.034043	$\frac{6}{Ж}\bar{W}_{151}$	-0.055200
		$-\frac{24}{Ж^2}\bar{W}_{040}W_{222}$	0.025298
		$\frac{4}{Ж}W_{311}\bar{u}'^2$	0.018905
		$-\frac{32}{Ж^2}\bar{W}_{040}W_{220}$	-0.016739
		$-\frac{3}{Ж}\bar{W}_{131}\bar{u}'^2$	-0.009523
		$-\frac{8}{Ж^2}\bar{W}_{131}W_{311}$	0.000863
		$\frac{3}{Ж^2}\bar{W}_{131}\bar{W}_{131}$	0.000217
Total	-0.711934		0.343373

As expected, the major contribution to the deviation from the $\cos^4$-law comes from the pupil coma and distortion. However, since the distortion is small and pupil coma is proportional to the distortion, the ability to manipulate the relative illumination through these terms is limited. The products of residual field curvature, astigmatism, and pupil-spherical-aberration contribute significantly to the change in relative illumination of a mobile lens to fourth-order and

may provide an effective degree of freedom during the lens design process. The relative illumination curves calculated with real ray tracing and using Eq. 24 are presented in Fig. 9. The plot shows excellent agreement between real ray tracing and the analytical solution over the entire FOV, confirming that our assumptions are still valid for relatively fast lenses with relatively large FOVs.

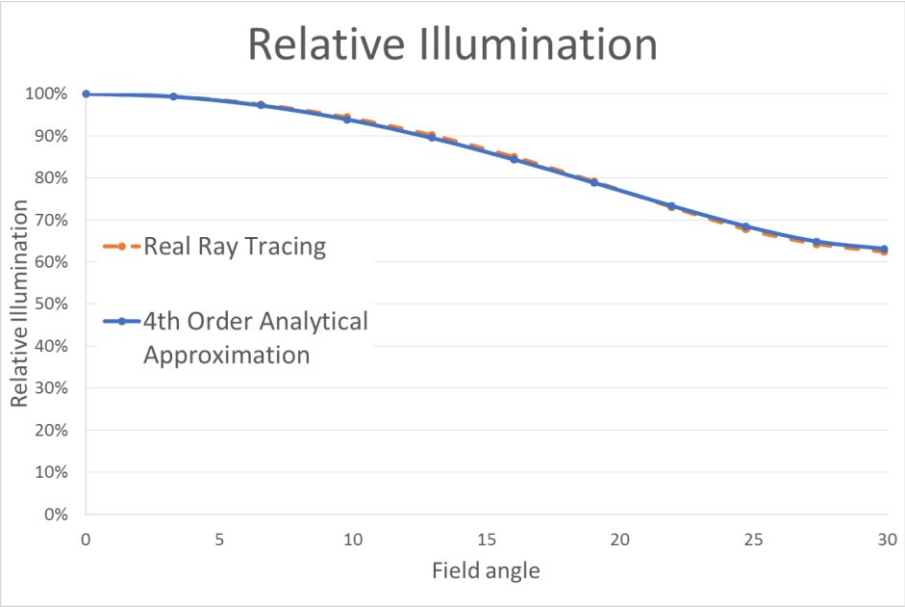

Figure 9. Relative illumination plot for U.S. Patent 6441971. Analytical equation and real ray tracing calculation show excellent agreement over the entire FOV.

4.2 Wide Angle Lens

The field of view of a wide angle objective that follows the $\cos^4$-law is limited to approximately 95°-105° due to a sharp decrease in illumination at the margin of the image. In US. Patent 2516724, shown in Fig. 10a, the decrease in the illumination follows the $\cos^3$-law and this makes it possible the widening of the angle of view up to 120° or more. In this design the area of the entrance pupil increases towards the edge of the field of view approximately by the factor of two, and as the result, the area of oblique beams entering the objective differs negligibly from the area of the axial beams. The author explains this phenomenon by maximum divergence from Abbe's conditions of sines for the front half of the objective with an object located in the plane of the diaphragm, or in other words, by maximizing pupil coma for the front half of the objective as shown in Fig. 10b [10].

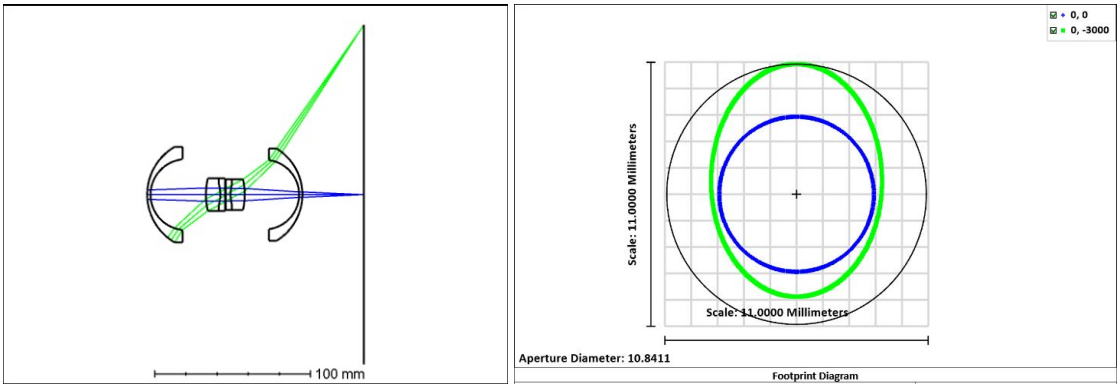

(a) (b)

Figure 10. U.S. 2516724: (a) Layout, (b) beam footprints at the exit pupil. The wide-angle objective consists of two nearly symmetrical halves. The form of the greatly curved exterior meniscus lens elements is of great importance. These meniscus lenses contribute substantial pupil coma, which increases the pupil area for oblique beams.

Aberration theory allows quantifying the required amount of pupil coma to achieve the $\cos^3$-law decrease in illumination. Similarly to Eq. 9, we use Taylor series expansion to show that to the fourth order of approximation, the cosine-to-the-third-power of the angle in the object space is given by

$$\cos^3(\theta) = [1 - \frac{3}{2}\cdot\bar{u}^2(\vec{H}\cdot\vec{H}) + \frac{15}{8}\cdot\bar{u}^4(\vec{H}\cdot\vec{H})^2]. \tag{32}$$

US. Patent 2516724 consists of two more or less symmetrical halves. If we assume that two halves are exactly symmetrical, Eq. 31 can be used to predict relative illumination of this lens. In a symmetrical lens the paraxial chief ray slope in object and image spaces are equal. The value of fourth- and six-order pupil coma are calculated by setting Eq. 31 equal to Eq. 32 and solving the following system of equations:

$$\begin{gathered} -2\bar{u}'^2 + \frac{4}{\mathcal{H}}\bar{W}_{131B} = -\frac{3}{2}\bar{u}^2 \\ 3\bar{u}'^4 + \frac{6}{\mathcal{H}}\bar{W}_{151B} - \frac{3}{\mathcal{H}}\bar{W}_{131B}\bar{u}'^2 + \frac{3}{\mathcal{H}^2}\bar{W}_{131B}\bar{W}_{131B} = \frac{15}{8}\bar{u}^4 \\ \bar{u}' = \bar{u}\,. \end{gathered} \tag{33}$$

The term $\frac{3}{\mathcal{H}^2}\bar{W}_{131B}\bar{W}_{131B}$ is small and can be neglected. We use the image pupil relationship in Eq. 25 and the fact that distortion in a symmetrical optical system is zero, to estimate the required amount of pupil coma to be

$$\bar{W}_{131B} = \frac{\mathcal{H}}{8}\bar{u}^2 \tag{34}$$

$$\bar{W}_{151B} = -\frac{\mathcal{H}}{8}\bar{u}^4\,. \tag{35}$$

It is interesting to note that an objective lens that satisfies Eq. 34 also meets the Hershel condition for the object located in the plane of the pupil [16], and therefore follows the decrease in the illumination according to the $\cos^3$-law to second-order.

In Fig. 11, we show relative illumination curves calculated with real ray tracing alongside the analytical solution. Since the analytical solution provides a fourth-order approximation to relative illumination, there is excellent agreement with real ray tracing calculation up to about 20° half field angle. The fourth order approximation in this case does not describe the relative illumination precisely enough for larger field angles.

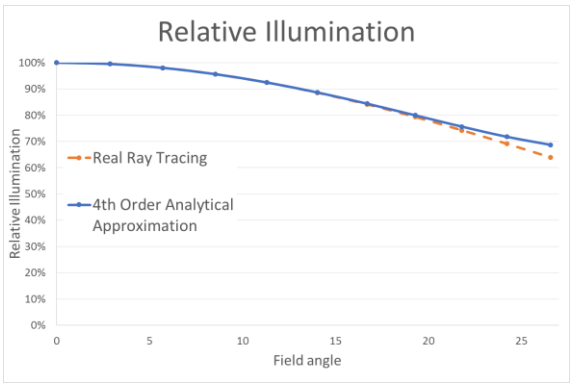

Figure 11. Relative illumination plot for U.S. Patent 2516724. Analytical fourth-order approximation and real ray tracing calculation show excellent agreement up to about 20° half field angle.

4.3 Optimization for a Target Relative Illumination

The analytical solutions presented in this paper allow efficient optimization for a desired relative illumination during the lens design process. A straightforward way to calculate the relative illumination in a lens design program is to determine the exit pupil area by tracing the rays in reverse from the image point in the direction cosines space. The relative illumination is proportional to the area of the pupil or to the number of rays that pass through the system [12]. Although this method is precise, the numerical integration requires tracing a large number of rays and therefore significantly slows down the optimization. On the other hand, we calculate the wave aberration coefficients by tracing only two first-order rays and estimate the relative illumination over the entire field of view of a lens.

We demonstrate that the fourth-order approximation to the relative illumination is sufficiently accurate for practical purposes and can be used, for example, to design a lens that has uniform illumination over the field. The objective being modified is a Double Gauss lens that operates at f/4 and has a FOV of 40°. We limit the distortion to be <5% and target both second- and fourth-order relative illumination coefficients to zero. The resulting system layout and relative illumination plot are shown in Fig. 12. The image is equally illuminated over its entire area.

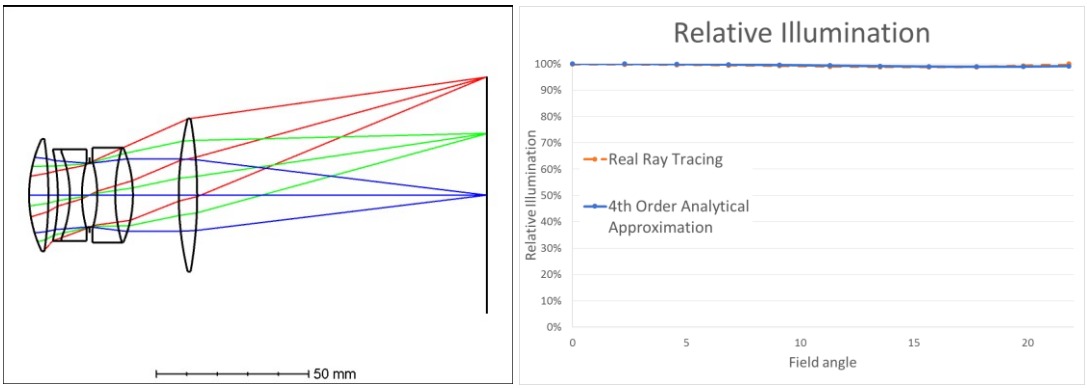

Figure 12. A Double Gauss lens was reoptimized while targeting both second- and fourth-order relative illumination coefficients to zero. The fourth-order approximation is sufficiently accurate for practical purposes and allows efficiently optimizing for a desired relative illumination during the lens design process.

5. CONCLUSION

Among other image quality requirements, the relative illumination may have a strong impact on the performance of a lens. A number of authors have shown that the standard $\cos^4$-law of illumination fall off is not accurate for an objective with image and pupil aberrations. However, a detailed and comprehensive investigation of the relation between relative illumination and individual aberration coefficients to fourth-order has not been previously discussed.

In this paper, the problem has been approached from the aberration theory point of view. An irradiance transport equation provides the irradiance changes at the exit pupil of the optical system, given the irradiance at the entrance pupil

and the pupil aberration function. We use this irradiance transport equation to derive a closed form solution that approximates the image illumination fall-off and accounts for the illumination effects of aberrations in an unvignetted optical system.

We consider three different possible aperture stop positions: as the last element, as the first element and between components of the lens system. Only the piston irradiance term is considered in the derivation, which is equivalent to the specification of a small diaphragm. Eq. 15, Eq. 24 and Eq. 30 give the relative illumination to the fourth-order of approximation in terms of aberration coefficients for each case respectively. A macro program for calculating the wave aberration coefficients to sixth-order is provided by Sasian [16]. If the aperture stop of the system follows the lens, only third-order distortion contributes to the fourth-order relative illumination coefficient. On the other hand, if the aperture stop precedes the lens, both image and pupil aberration affect the relative illumination. In this case, it is possible to have sufficient pupil aberrations such that the illumination will be more uniform or even constant over the entire field. If the aperture stop is located between the components of the lens, we need to consider image and pupil aberration contributions of the rear half and distortion of the front half of the objective. This result reveals a new path to improve image quality and required illumination by balancing aberrations of the two halves.

In several special cases, it is possible to come up with a more compact, reduced form of the equations. Table 1 summarizes second- and fourth-order relative illumination coefficients for different cases. The results are validated with real ray tracing. The agreement to eighth digits of precision adds support the correctness of the formulas.

Finally, we provide several examples of lenses that instead of the $\cos^4$-law show improved illumination at the focal plane. Aberration theory is used to provide insight into the role of individual aberration coefficients on the relative illumination of these lenses. Although the specification of a small diaphragm was used in the derivation, this approximation has shown to be sufficiently accurate for practical purposes.

Our future research on the irradiance transport in a lens system will involve derivation of other fourth-order irradiance coefficients in terms of wave aberration coefficients. If all fourth-order irradiance terms are considered, it will be possible to analytically calculate the relative illumination more accurately for a lens system with a finite aperture; however, we expect that the equations will become too complex to provide any additional intuitive insight.

The analytical results described in this manuscript serve to advance the state-of-the-art tools for the aberration analysis of optical imaging systems and enhance the optics community's collective understanding of the role of aberrations in the irradiance and illumination of optical systems.

REFERENCES

[1] J. Petzval, "Professor Petzval New Lens," Photographic Notes, pp. 118-121 (1858)
[2] M. von. Rohr, "Distribution of light on the focal plane of a photographic objective," Zeitschr. Insttrymentenk. 18, pp. 171-180 and 197-205 (1898)
[3] T. R. Dallmeyer, "Technical meeting," Photographic Journal, Vol 19., pp. 221-232 (1895)
[4] F. E. Washer, "Characteristics of wide-angle airplane camera lenses," Journal of Research of the National Bureau of Standards, Vol. 29, pp. 233-246 (1942)
[5] J. M. Palmer and B. G. Grant, "The Art of Radiometry," SPIE Press (2010)
[6] M. Reiss, "The $\cos^4$ Law of Illumination," Journal of Optical Society of America, Vol. 35, N. 4, pp. 283-288 (1945)
[7] M. Reiss, "Notes on the $\cos^4$ Law of Illumination," Journal of Optical Society of America, Vol. 38, N. 11, pp. 980-986 (1948)
[8] I. C. Gardner, "Validity of the Cosine-Fourth-Power Law of Illumination," Journal of Research of the National Bureau of Standards, Vol. 39, pp. 213-219 (1947)
[9] F. Wachendorf, "The Condition of Equal Irradiance and the Distribution of Light in Images Formed by Optical Systems without Artificial Vignetting," Journal of Optical Society of America, Vol. 43, N. 12, pp. 1205-1208 (1953)
[10] M. M. Roossinov, "Wide angle orthoscopic anastigmatic photographic objective," US 2516724 (1950)
[11] H. H. Hopkins, "Canonical and Real-Space Coordinates Used in the Theory of Image Formation," Applied Optics and Optical Engineering, Vol. 9, Chap. 8 (1983)
[12] M. P. Rimmer, "Relative illumination calculations," Proc. SPIE, Vol. 655, pp. 99-104 (1986)

[13] Zemax LLC., “OpticStudio Manual” (2016)
[14] J. Sasian, “Theory of six-order wave aberrations,” Applied Optics, Vol. 49, No. 16 (2010)
[15] C. Roddier and F. Roddier, “Wave-front reconstruction from defocused images and the testing of ground-based optical telescopes,” J. Opt. Soc. Am. A, Vol. 10, No. 11 (1993)
[16] J. Sasian, “Introduction to Aberrations in Optical Imaging Systems,” Cambridge University Press (2013)
[17] J. Sasian, “Interpretation of pupil aberrations in imaging systems,” SPIE Proceedings, Vol. 6342 (2006)
[18] R. Kingslake, “Lens Design Fundamentals,” Academic Press, second edition (2010)
[19] D. Reshidko and J. Sasian, “Optical analysis of miniature lenses with curved imaging surfaces,” Appl. Opt. 54 (28), pp. E216–E223 (2015)
[20] A. Ning, “Compact lens with external aperture stop,” US 6441971 B2 (1999)